The Wind Energy Potential of Iceland

Nawri, Nikolai; Petersen, Guðrún Nína ; Björnsson, Halldór ; Hahmann, Andrea N.; Jónasson, Kristján ; Hasager, Charlotte Bay; Clausen, Niels-Erik

Published in:
Renewable Energy

Link to article, DOI:
10.1016/j.renene.2014.03.040

Publication date:
2014

Document Version
Publisher's PDF, also known as Version of record

Renewable Energy 69 (2014) 290–299

Contents lists available at ScienceDirect

Renewable Energy

journal homepage: www.elsevier.com/locate/renene

The wind energy potential of Iceland

Nikolai Nawri [a,*], Guðrún Nína Petersen [a], Halldór Bjornsson [a], Andrea N. Hahmann [b], Kristján Jónasson [c], Charlotte Bay Hasager [b], Niels-Erik Clausen [b]

[a] Icelandic Meteorological Office, Bústaðavegur 7–9, 150 Reykjavik, Iceland
[b] DTU Wind Energy, Technical University of Denmark, Risø Campus, 4000 Roskilde, Denmark
[c] Faculty of Industrial, Mechanical Engineering and Computer Science, University of Iceland, 107 Reykjavik, Iceland

ARTICLE INFO

Article history:
Received 17 October 2013
Accepted 21 March 2014
Available online

Keywords:
Wind energy potential
Wind atlas
Mesoscale modelling
Wind resource mapping
Iceland

ABSTRACT

Downscaling simulations performed with the Weather Research and Forecasting (WRF) model were used to determine the large-scale wind energy potential of Iceland. Local wind speed distributions are represented by Weibull statistics. The shape parameter across Iceland varies between 1.2 and 3.6, with the lowest values indicative of near-exponential distributions at sheltered locations, and the highest values indicative of normal distributions at exposed locations in winter. Compared with summer, average power density in winter is increased throughout Iceland by a factor of 2.0–5.5. In any season, there are also considerable spatial differences in average wind power density. Relative to the average value within 10 km of the coast, power density across Iceland varies between 50 and 250%, excluding glaciers, or between 300 and 1500 W m^{-2} at 50 m above ground level in winter. At intermediate elevations of 500–1000 m above mean sea level, power density is independent of the distance to the coast. In addition to seasonal and spatial variability, differences in average wind speed and power density also exist for different wind directions. Along the coast in winter, power density of onshore winds is higher by 100–700 W m^{-2} than that of offshore winds. Based on these results, 14 test sites were selected for more detailed analyses using the Wind Atlas Analysis and Application Program (WAsP).

1. Introduction

In Iceland, more than 80% of the primary energy supply derives from geothermal and hydropower. Almost all electricity produced in Iceland derives from renewable sources, with 73% from hydropower plants, and 27% from geothermal plants [1]. One aspect of hydropower in Iceland is that the streamflow in rivers tends to exhibit a large annual variation, with larger flow during summer than in winter. Since the annual cycle of wind in Iceland has the opposite phase, with stronger winds in winter than in summer, wind power can potentially be used effectively in combination with hydropower.

In coming decades it is expected that glacier melt will increase the hydropower potential in Iceland [2], with the increase in runoff peaking in the latter half of this century [3]. Analysis of likely changes in wind climate [4,5] does not reveal such large scale changes for the wind, and thus wind energy production may in the longer term prove to be more sustainable.

The use of wind power for electricity generation in Iceland has hitherto been limited to small wind turbines for off-grid use, and until recently there were no large wind turbines in operation in Iceland. Despite Iceland having a favourable climate for wind power [6], detailed research into the wind power potential in Iceland is quite recent.

The goal of this study therefore is to develop a wind atlas for Iceland, to provide the first overview across the entire island of the statistics relevant to wind energy assessments. Based on model data that has been corrected using surface station wind measurements, we estimate the statistical parameters describing local wind speed distributions across Iceland. This allows us to make a regional comparison of wind energy potential within Iceland and also to identify possible sites for wind farms. This study is part of the Nordic IceWind project, which focuses on wind engineering in cold climates and aims to improve forecast of wind, waves, and icing.

The structure of the paper is as follows: In Section 2 we describe the data used and methodology. In Section 3 we provide an overview of wind power potential across Iceland. In Section 4 we discuss the results of a more detailed assessment of 14 test sites, followed by our conclusions.

* Corresponding author. Tel.: +354 522 6000; fax: +354 522 6001.
E-mail address: nikolai@vedur.is (N. Nawri).

http://dx.doi.org/10.1016/j.renene.2014.03.040

2. Methodology

2.1. Wind modelling

The Icelandic network of weather stations is sufficient to provide a good overview of the surface wind conditions over the low-lying parts of the country. However, it leaves several regions unobserved, which may be suitable for the installation of wind farms. It is therefore important to augment the observational data with results from numerical simulations, which provide regularly gridded fields of atmospheric variables at different heights above the ground.

The simulated data used for this study was obtained from the Institute for Meteorological Research in Iceland. The numerical model data was produced with the mesoscale Weather Research and Forecasting (WRF) Model (Version 3.1.1; see Skamarock et al. [7] for details). Simulations were performed in three nested horizontal domains, all approximately centred around Iceland: the outer domain with 43 × 42 grid points spaced at 27 km, the intermediate domain with 95 × 90 grid points spaced at 9 km, and the inner domain with 196 × 148 grid points spaced at 3 km. As shown in Fig. 2, the northwest corner of the outer domain covers a part of the southeast coastal region of Greenland. However, the main landmass included in the model domain is Iceland. The data used here is that of the inner domain. The initial and boundary conditions for the model simulations were determined by 6-hourly operational analyses obtained from the European Centre for Medium-Range Weather Forecasts (ECMWF) [8,9], valid at 00, 06, 12, and 18 UTC. After initialisation of the model run, this data is only applied at the outer boundaries. WRF model output fields were produced every 3 h in one continuous simulation, with a 15-day spin-up period. Data is available for the period 1 Sep 1994–2 Nov 2009. However, to include only years with complete data records, the main analysis here is limited to the 1995–2008 period.

With a grid-point spacing of 3 km, the WRF model results are too coarse for a precise assessment of the wind conditions within a limited region, such as an individual valley or ridge, that may be appropriate for wind energy production. For this, a spatial resolution of 100 m or higher is required, a resolution that is not practical to use with a prognostic numerical model. Here, instead the Wind Atlas Analysis and Application Program (WAsP), developed by the Wind Energy and Atmospheric Physics Department at Risø National Laboratory (now the Department of Wind Energy at the Technical University of Denmark), was used for more detailed analyses of the wind energy potential of selected sites. WAsP employs parameterised boundary-layer modelling within a geographically consistent or contained region [10,11]. The input data can be either measured or simulated wind speed and direction time-series at one location somewhere within the domain, but ideally at a

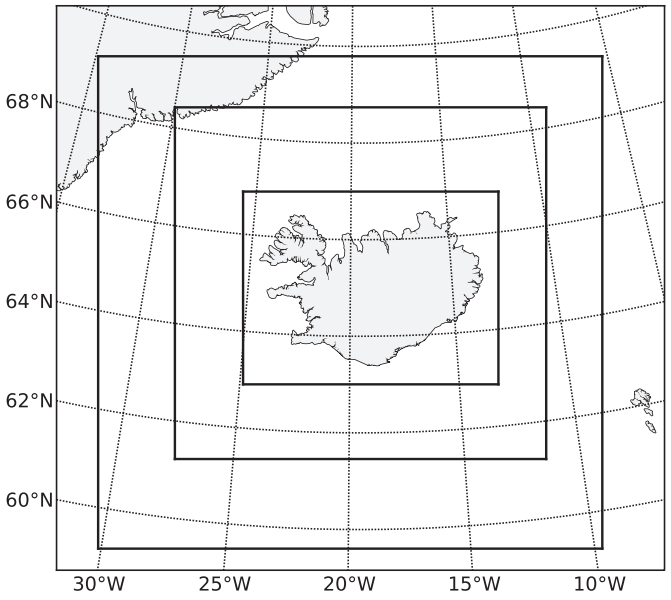

Fig. 2. Boundaries of the three nested WRF model domains.

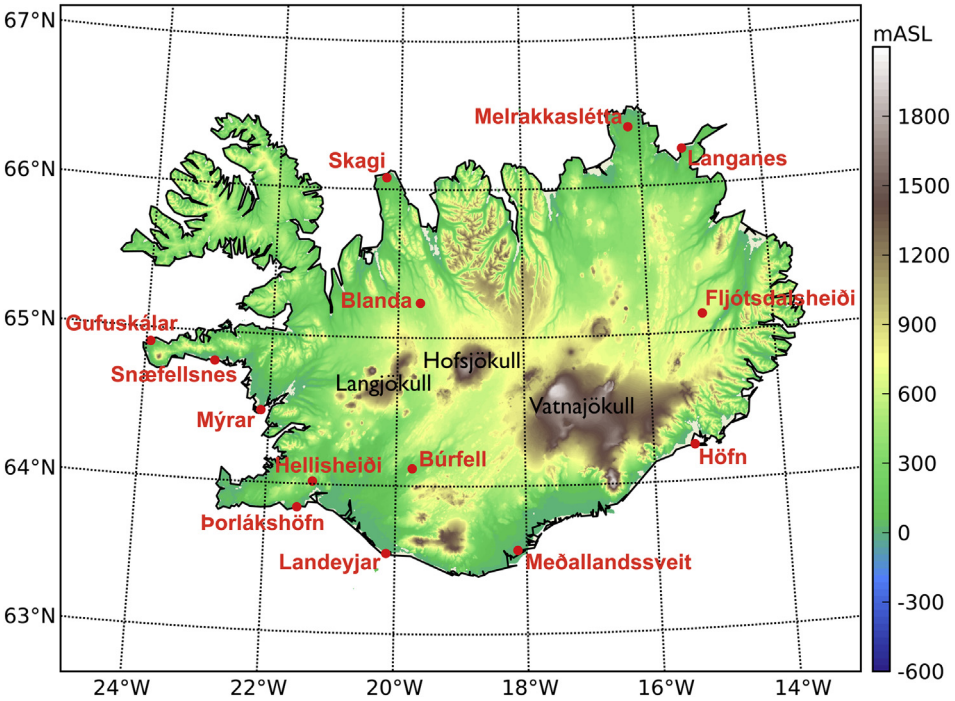

Fig. 1. Topographic map of Iceland, with the locations of sites, for which detailed analyses were performed, shown in red. (For interpretation of the references to colour in this figure legend, the reader is referred to the web version of this article.)

representative location. The methodology of running WAsP with input from a numerical mesoscale model is well established. Frank and Landberg [12], Mengelkamp et al. [13], Mengelkamp [14], Frank et al. [15] used data from the Karlsruhe Atmospheric Mesoscale Model (KAMM), whereas Tammelin et al. [16] used data from the Applications of Research to Operations at Mesoscale (AROME) model.

In the first step of WAsP, a "generalised" wind climate is created through a process of reverse (or "upward") modelling. This step is intended to remove effects of local terrain features and obstacles from measured wind data, or of model orography and surface type from simulated winds. The result is a wind climate for the entire WAsP domain, which is an approximation of the wind above the boundary layer. One of the main assumptions made is a near-neutral stability stratification of the boundary layer atmosphere. The vertical dependence of wind speed is therefore assumed to follow a logarithmic profile, with a small heat flux modification. The response of vertical wind shear to spatial differences in surface roughness is taken into account. Other parameterisations of boundary-layer wind conditions employed in WAsP are a geostrophic drag law, balancing pressure gradients against frictional forces; a simplified description of orographic effects, assuming potential flow, with a viscous modification in a shallow surface layer; as well as a description of sheltering for objects with sizes comparable to the height above ground of the input data, and for distances from the input data comparable to the object size [10,11]. The wind conditions at any point within the domain, at the same or different heights above the ground, are derived from the generalised wind climate through direct (or "downward") modelling, by considering the specific geographical conditions at the target location.

The accuracy of the projected wind climate depends on the homogeneity of the overlying flow and the complexity of the geographical conditions within the domain. Due to the simplified description of boundary-layer dynamics, there are limitations [17,18]. In addition to reliable reference data, accurate high-resolution topography and surface type classification are required. Furthermore, winds at different locations within the domain have to be well correlated within the analysis period [19]. This requires that buoyancy effects are small, and that the terrain is sufficiently smooth to allow for essentially laminar flow. Also, different parts of the domain should not be separated by orographic barriers. For example, measurements in one valley cannot be assumed to be correlated well with the wind conditions in a neighbouring valley.

2.2. Weibull statistics

Following the established practices of the WAsP method, averages and other relevant statistical properties are calculated here from an analytical approximation of the wind speed distribution, rather than from the data directly.[1] Of the various probability density functions for boundary-layer wind speeds, U, the 2-parameter Weibull distribution,

$$f(U;A,k) = \frac{k}{A}\left(\frac{U}{A}\right)^{k-1}\exp\left[-\left(\frac{U}{A}\right)^{k}\right], \quad (1)$$

is the one most commonly employed for wind energy studies [20]. It is determined by the scale parameter $A \geq 0$ in units of wind speed, and the non-dimensional shape parameter $k \geq 1$. By its definition, the Weibull distribution is only applicable to non-zero wind speeds. Calm conditions are therefore excluded from the analysis. There are different methods for determining the parameters A and k from a given measured distribution [21,20]. For wind energy assessments, the interest is primarily on high wind speeds. Therefore, following the method employed by Troen and Petersen [10] and Petersen et al. [11], the two Weibull parameters are calculated here by: 1) matching the mean cubed wind speed in the Weibull distribution to that of the measured or modelled distribution of wind speeds; and 2) requiring the occurrence of above average wind speeds in the Weibull distribution to be equal to that of the measured or modelled distribution.

Throughout Iceland, the average difference between seasonal mean wind speed calculated from the Weibull fit and that calculated directly is 0.08 m s^{-1} (0.04 m s^{-1}) in winter (summer) for station data, and −0.10 m s^{-1} (−0.02 m s^{-1}) in winter (summer) for WRF model data. Overall, there is therefore a small positive bias of the Weibull fits compared with measurements, and a small negative bias compared with model data. Mean absolute differences are 0.10 m s^{-1} (0.05 m s^{-1}) in winter (summer) for station data, and 0.15 m s^{-1} (0.05 m s^{-1}) in winter (summer) for WRF model data. This amounts to 1–2% of the directly calculated averages.

Once the two Weibull parameters have been determined, the average of the (wind speed) distribution is given by

$$\mu = A\,\Gamma(1+1/k), \quad (2)$$

where Γ denotes the gamma function.

Wind power density, a measure of the energy flux through an area perpendicular to the direction of motion, varies not only with the cube of wind speed, but also with air density. To simplify wind energy assessments, and to allow for the use of Weibull statistics, it is commonly assumed that air density, ρ, is not correlated in time with wind speed throughout the averaging period [22]. Average wind power density is then proportional to the mean cube of wind speed,

$$E = \frac{1}{2}\,\overline{\rho}\,A^3\,\Gamma(1+3/k), \quad (3)$$

where $\overline{\rho}$ is the average air density. Wind power density only depends on atmospheric variables, and is therefore most appropriate for turbine-independent evaluations of wind energy potential.

To be able to determine the actual power or energy, which can be extracted from the air, specific information about a chosen wind turbine is required. The turbine considered in this study is the Enercon E44 (900 kW) with a hub height of 55 m. This was chosen, since the Icelandic power company Landsvirkjun is currently in the process of testing two of these turbines near the Búrfell hydroelectric power station. The available power not only depends on the area swept by the rotor blades, but also on aerodynamic efficiency. Since the wind is not entirely stopped by the turbine, only a certain proportion of the incoming power can be extracted, which depends on the number, size, and shape of the blades, as well as on wind speed. This efficiency is expressed by a turbine-specific power coefficient, which has a theoretical maximum of 0.593 [23]. Practically, however, the power coefficient of modern wind turbines typically has highest values of 0.40–0.50, for wind speeds between 5 and 10 m s^{-1}. The effective power curve, i.e., the actual power produced by a given turbine as a function of wind speed, needs to be determined empirically, and is made available by the manufacturers. For a particular turbine, the average available wind power can then be calculated by integrating over its power curve, multiplied by the probability density function for wind speed, as determined by the Weibull distribution.

[1] Wind speed here is always referring to the horizontal motion of the atmosphere, ignoring any vertical displacements. With wind turbines rotating in a vertical plane, this is the component of the three-dimensional flow relevant for wind energy assessments.

For any given turbine, there are three important characteristic wind speeds. The cut-in speed is the lowest wind speed at which a turbine can generate usable power. The rated speed (typically between 12 and 16 m s^{-1}) is the lowest wind speed at which a turbine operates at its rated capacity, i.e., at maximum power output. The cut-out speed is the lowest wind speed at which there is the potential of damage to the turbine, if operation continues. At wind speeds between the rated and cut-out speed, power production of pitch-regulated variable-speed turbines, as those considered here, is kept as close to the rated capacity as possible. This is achieved by rotating each blade around its longitudinal axis, to reduce aerodynamic lift or drag, while maintaining maximum power output. The relative angle of attack by the wind on the blades can either be increased (as in stalling) or decreased (as in feathering). At the cut-out speed (typically between 20 and 30 m s^{-1}), mechanical breaks may need to be employed in addition to pitch control, to bring the rotor to a standstill. Consequently, no energy is produced at this and higher wind speeds.

2.3. Density effects

As mentioned in the previous subsection, wind power density depends linearly on air density which, for simplicity, is assumed to be uncorrelated with wind speed throughout the averaging period. The standard density value used for wind energy assessments, such as in WAsP, is $\rho_0 = 1.225$ kg m^{-3}, which corresponds to dry air with a temperature of 15 °C and a pressure of 1013.25 h Pa.

In the case of Iceland, model results and measurements show that, at a given location, seasonal air density changes are small, justifying the use of a constant air density value for the calculation of average power density. For the coastal region of Iceland, the differences between winter and summer averages are around 2%, and smaller at higher elevations. However, given the large range in terrain elevation, spatial air density differences are around 25% between coastal regions and the highest points over the glaciers, and around 13% within that part of the island with terrain up to 1000 m above mean sea level (mASL). The exponential decrease in pressure with altitude outweighs the linear decrease in temperature, leading to an effective decrease in air density with height. The increase in wind speed or wind power, that is usually found with terrain elevation or turbine height, is therefore somewhat mitigated by a decrease in air density. In Iceland, the standard value of 1.225 kg m^{-3} is only appropriate at low elevations, and at heights above the ground of up to 100 m, where the effects of reduced temperature and pressure relative to standard atmospheric conditions approximately cancel each other. Over the interior of the island, at elevations below 1000 mASL, air density varies between 1.05 and 1.20 kg m^{-3}. The correction of monthly, seasonal, and annual wind power values, originally calculated with standard air density, is done here through multiplication with the ratio $\rho(x,y,z)/\rho_0$, where $\rho(x,y,z)$ is the appropriate mean field of air density.

3. Results and discussion

3.1. Evaluation of mesoscale model results

Fig. 3 (left panel) shows a comparison of average wind speed at 10 mAGL between the WRF model and station measurements during winter. Interpolated model data values at station locations are determined by inverse distance weighted averages from the four surrounding grid-points, if these grid-points are all over land, according to the model land-sea mask. Along the coast, if any of the surrounding grid-points are over the ocean, the nearest land grid-point value is used. The differences along the coast range from 0 to 2.5 m s^{-1}. The bias (model minus measurements) in the interior of the island is larger in magnitude and negative, with differences between simulated and measured averages as low as −4.5 m s^{-1} at station locations, and possibly lower over the glaciers, where no measurements are available. During the rest of the year (not shown), the differences are smaller, as absolute wind speeds are reduced. Wintertime differences in average wind power density at 10 mAGL (not shown) are up to 750 W m^{-2} along the coast, and as low as −750 W m^{-2} at station locations in the interior. These differences are of about half the magnitude of the measured values. The negative bias in the intensity of low-level winds over the land is most likely due to too large surface roughness in the model setup. Due to the absence of tall vegetation in most parts of Iceland, local surface roughness lengths should generally be 1–3 cm, or less. Nonetheless, in the model setup, these values are exceeded by up to an order of magnitude at many grid points.

Due to the systematic nature of the low-level wind speed bias, differences between measured and simulated averages can be reduced by rescaling the model data, i.e., by multiplying the grid-point time-series with a non-dimensional positive factor. Within each averaging period, this transformation only depends on the location in space, and preserves the percentage of zero wind speeds, or calm conditions. With one free parameter at each grid point, this allows for the correction of one statistical property.

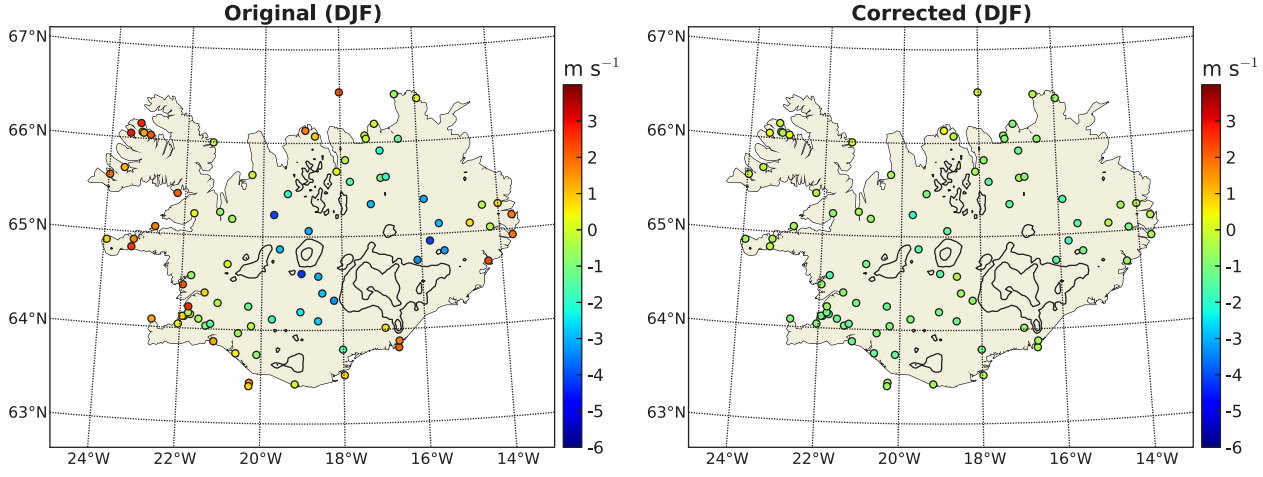

Fig. 3. Differences in winter (DJF) averages of wind speed at 10 mAGL between either original or corrected WRF model data and station measurements (model minus measurements). Terrain elevation contour lines are drawn at 1000 and 1500 mASL.

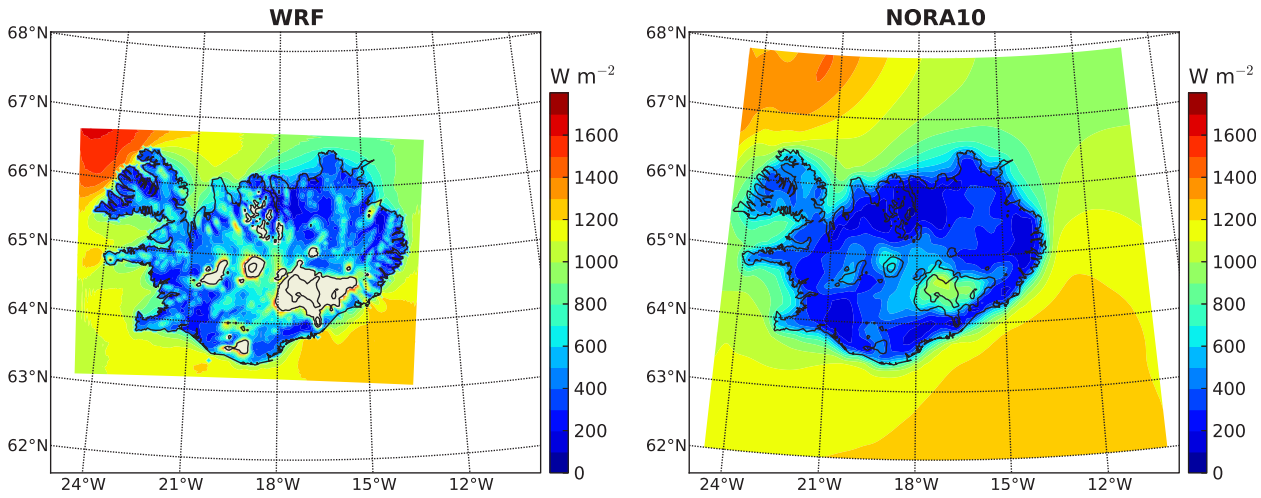

Fig. 4. Annual average wind power density at 50 mAGL, based on corrected WRF model and NORA10 data. WRF model values above 1000 mASL are masked.

For wind energy assessments, the main emphasis is on an accurate determination of average wind power density. As discussed in the previous section, average power density is approximately proportional to the mean cube of wind speed. Rescaling factors for modelled wind speed time-series U_m, interpolated to station locations, are therefore defined here as $\sqrt[3]{\overline{U_o^3}/\overline{U_m^3}}$, where U_o are the measured time-series, and the bars indicate temporal averages. Rescaling factors determined at station locations are interpolated onto the horizontal model grid through inverse distance-weighted horizontal averaging, whereby the half-width of the exponential weighting function, at each grid-point, is set equal to the distance to the nearest station. Only stations with at least 95% wind speed data availability within the study period are considered. Although this correction is aimed at mean cubed wind speed, differences between modelled and measured mean surface wind speeds are significantly reduced as well (see right panel in Fig. 3). Since wind speed measurements are only available at 10 mAGL, rescaling factors at greater heights above the surface are applied such that the values determined at 10 mAGL linearly decrease to zero at 300 mAGL, which is taken as the average gradient height.

Since measurements are also only available over the land, rescaling factors at ocean grid-points are set equal to one. Over the ocean, model results are evaluated against data from the Norwegian Reanalysis at 10 km spatial resolution (NORA10) [24]. NORA10 was derived by dynamical downscaling of the ECMWF reanalyses ERA-40 [25] until 2002, and the ECMWF operational analyses afterwards, using the High Resolution Limited Area Model (HIRLAM) version 6.4.2 [26]. NORA10 data is available for the entire study period. The WRF model and NORA10 datasets were obtained by downscaling the same boundary conditions, but using different models, with different spatial resolutions. A comparison between the annual average wind power density at 50 mAGL, based on corrected WRF model and NORA10 data, is shown in Fig. 4.[2] Despite differences in domain size and spatial resolution, power densities over the near-coastal ocean around Iceland are similar in the two datasets. The main differences exist in the northwest corner of the WRF model domain, where the gradient in wind speed between land and ocean, based on the WRF model, appears excessive. Most likely this is an artefact of lateral model boundary effects.

3.2. Climatological wind conditions

Winter (DJF) and summer (JJA) averages of wind speeds at 50 and 100 mAGL are shown in Fig. 5. The spatial variability of wind speed strongly depends on terrain elevation. Over intermediate terrain elevations of 500–1000 mASL, wind speeds at 50 mAGL vary over the course of the year between 6 and 8 m s^{-1} in summer, and 10–11 m s^{-1} in winter. The lowest wind speeds at some sheltered locations range from 3 m s^{-1} in summer to 5 m s^{-1} in winter. At 100 mAGL, the seasonal range of wind speeds over intermediate terrain elevations is between 7 and 9 m s^{-1} in summer, and 11–12 m s^{-1} in winter.

Two locations with the same average wind speeds may have very different wind speed distributions. At one location, predominantly low wind speeds, on average, may be compensated by extreme winds during occasional severe storms, whereas at the other location wind speeds fluctuate more closely around the average. In the former case, the average available power may be considerably lower than in the latter case, due to the higher occurrence of wind speeds below the cut-in limit, and above the rated speed. This ambiguity in the relationship between the averages of wind speed, power density, and available power needs to be taken into account when evaluating the wind energy potential of a given location.

Based on Weibull statistics, the shape of the wind speed distribution is described by parameter k. For $k = 1$, the distribution is exponential, with calm conditions having the highest occurrence. For $k = 2$, wind speed has a Rayleigh distribution, with the most frequent (modal) wind speeds below the average wind speed. Over flat terrain, this is a common situation, implying that the two horizontal vector components are uncorrelated in time, and are each normally distributed, with zero mean and the same variance [27]. For values of k around 3.5, the Weibull distribution is close to a normal distribution, for which the modal and average wind speed coincide. As shown in Fig. 6, the shape parameter across Iceland varies between 1.2 and 3.6 in winter, and between 1.2 and 3.2 in summer. In winter, values generally increase with height above ground, the opposite being true in summer.

Mean wind speed is related to the shape parameter, k, through the gamma function with argument $x = 1 + 1/k$ (see Eq. (2)). However, despite its spatial range of values, the effect of the shape

[2] In Iceland, almost 80% of the area above 1000 mASL is covered with glaciers. Due to the combined effects of high terrain and low surface roughness, average power density over glaciers is about twice as high as over intermediate terrain between 500 and 1000 mASL. However, since these regions are not accessible for wind energy production, WRF model values above 1000 mASL are masked in some of the figures, to allow for a more nuanced scaling at low values.

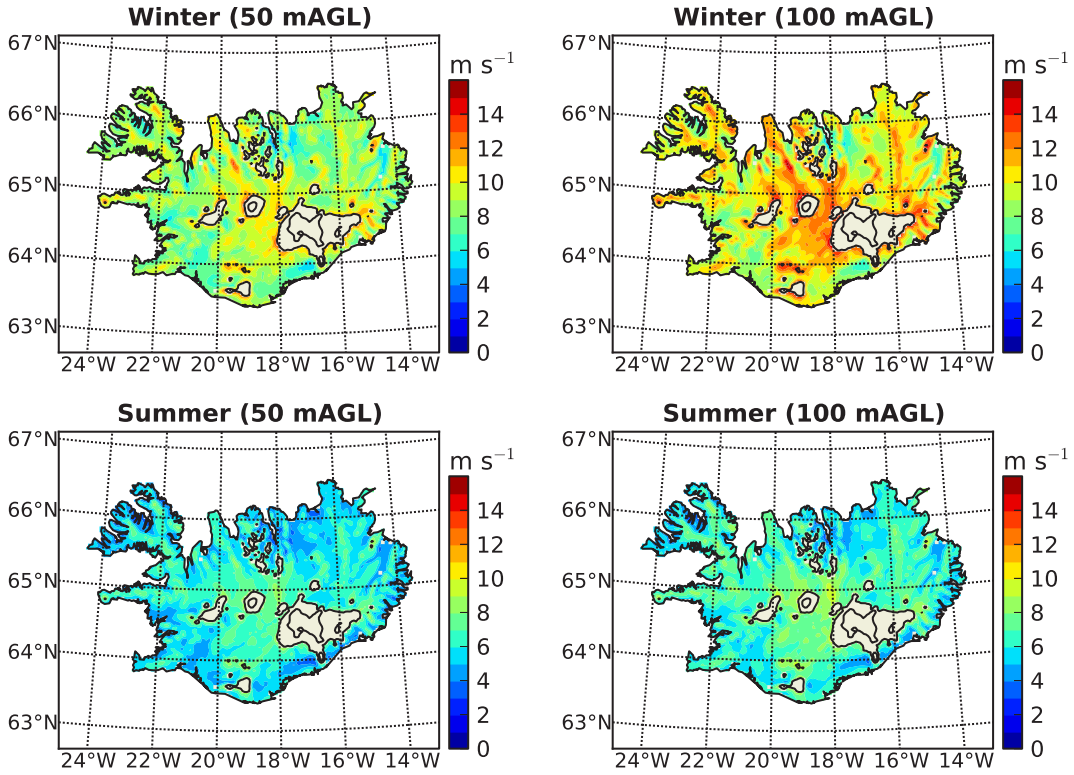

Fig. 5. Winter (DJF) and summer (JJA) averages of wind speed at 50 and 100 m above ground level, based on corrected WRF model data.

parameter on mean wind speed is negligible, since $\Gamma(1 + 1/k)$ fluctuates by only a few percent across Iceland. For annual time-series at 50 mAGL, it varies between 0.886 and 0.925. On the other hand, mean cubed speed, or average power density, is significantly affected by variations in k. It is related to the shape parameter through the gamma function with argument $1 + 3/k$ (see Eq. (3)). For annual time-series at 50 mAGL, $\Gamma(1 + 3/k)$ varies between 0.976 and 2.737 across the island.

3.3. Wind power density

Winter (DJF) and summer (JJA) averages of wind power density at 50 and 100 mAGL, based on corrected WRF model data, are shown in Fig. 7. Since power density depends on the cube of wind speed, the relative seasonal and spatial variability is significantly larger than that for average wind speed. Compared with summer, average power density in winter is increased throughout Iceland by a factor of 2.0–5.5, with the largest increases on the lower slopes of Vatnajökull, along the complex coastline of the Westfjords, and over the low-lying areas in the northeast. For comparison, average wintertime wind speeds only increase by a factor of 1.2–1.8, relative to summer (see again Fig. 5). In any season, there are also considerable spatial differences in average wind power density. Relative to the average value within 10 km of the coast, power density across Iceland varies between 50 and 450%. The largest reduction relative to the near-coastal average occurs in low-lying regions of the southwest and northeast. At intermediate elevations of 500–1000 mASL, independent of the distance to the coast, power density is within 200–250% of the near-coastal average. Again, for comparison, the spatial variability of wind speed throughout the year is between 75 and 225% of the average wind speed within 10 km of the coast.

In addition to seasonal and spatial variability, differences in average wind speed and power density also exist for different wind directions. On the large scale, without local terrain-induced effects, directional variability is usually due to the passage of fronts associated with cyclonic storm systems, causing sudden changes in wind speed and direction. Near the coast, thermal land–sea gradients, as well as the sharp transition in surface roughness and form drag between ocean and land, may cause differences between the intensity of onshore and offshore winds. In the presence of elevated terrain, there may be dynamically induced differences in the intensity of horizontally or vertically deflected flow, or between upslope and downslope winds.

Differences in average wind power density at 50 mAGL between winds from the southerly and northerly 30-degree sector (southerly minus northerly) are shown in Fig. 8. In panel (a), power density differences along the northern and southern coast of Iceland are shown as a function of longitude. Here, coastal grid points are defined as having a neighbouring land–sea mask value in the latitudinal direction of the opposite sign. The coastal zone is therefore a double line of grid points, one over the ocean, the other over the land. Along most of the northern coast in winter, power density of onshore winds is higher by 400–700 W m^{-2} than that of offshore winds. Based on annual wind statistics, the difference remains mostly positive, but is smaller than in winter. In summer, as overall wind speeds decrease, differences between the power density of onshore and offshore winds become small and unsystematic. Due to the large differences in terrain elevation along the south coast, power density differences between southerly and northerly winds there fluctuate more strongly with longitude than along the north coast. In winter, power density of onshore winds, for the most part, is higher by 100–700 W m^{-2} than that of offshore winds. However, in summer, the relative intensity of southerly and northerly winds changes, with northerly offshore winds becoming stronger at certain parts of the coast. This is due to the effects of downslope forcing by elevated coastal terrain. Power density differences between the southerly and northerly 30-degree sector, as a function of the south-to-north

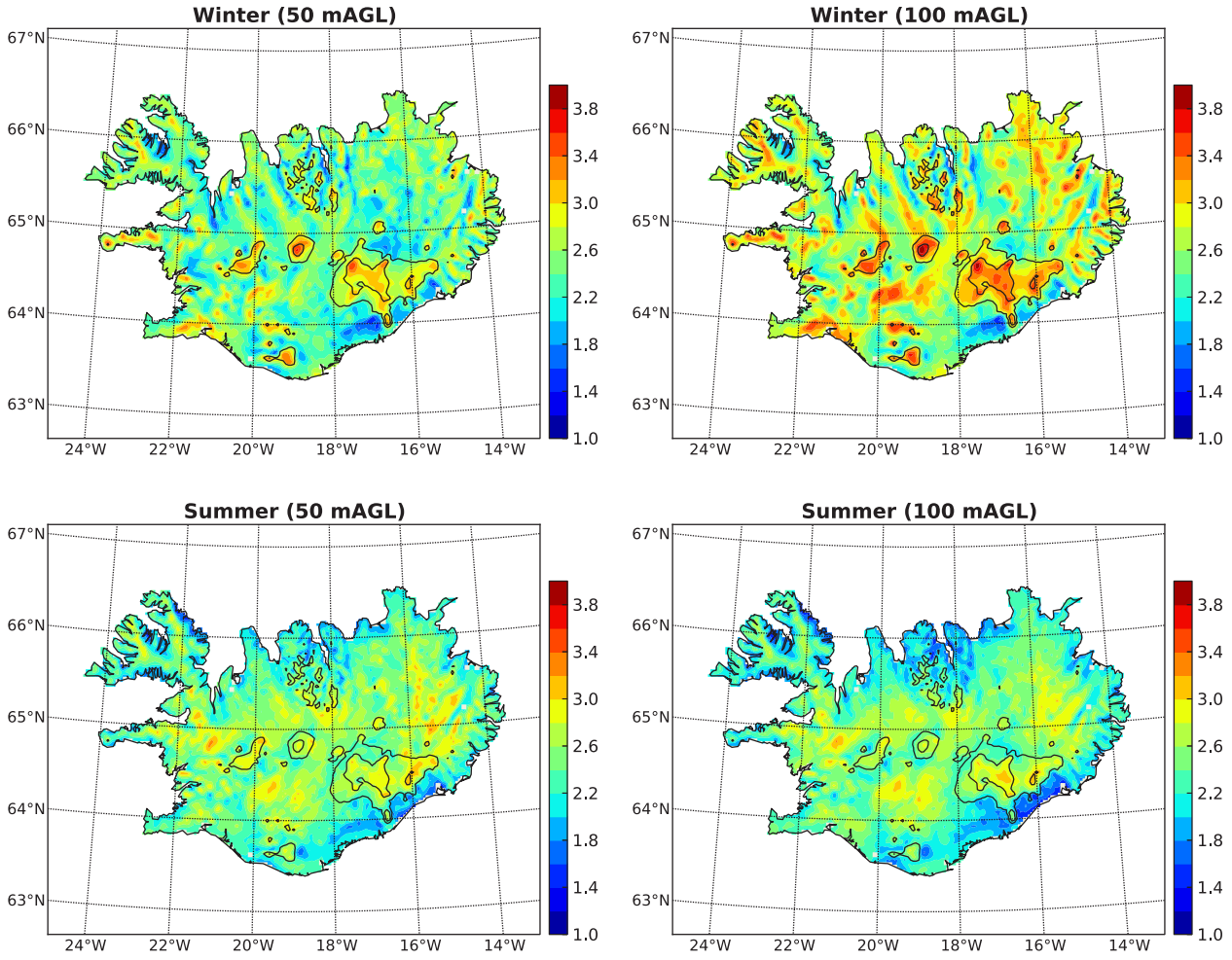

Fig. 6. Weibull shape parameter, *k*, for wind speed at 50 and 100 mAGL, and for all wind directions, based on corrected WRF model data.

terrain slope, are shown in panel (b). On average, across the island, power density of downslope winds is greater than that of upslope winds. When analysed on a horizontal map (not shown), the largest differences between the two wind direction sectors are associated with the main glaciers, Langjökull, Hofsjökull, Eyjafjallajökull, and Vatnajökull, where the strongest winds occur on the upper parts of lee slopes, as well as on the low-pressure side (left, facing downstream) of elevated terrain. Conversely, low-wind stagnation points are located on the lower parts of windward slopes. In these regions, local measurements are not available for direct comparisons. However, given the evidence from previous research, the modelled terrain effects appear to be at least qualitatively accurate.

Using atmospheric and wind tunnel measurements, as well as numerical simulations, studies of wind flow over elevated terrain under neutral or near neutral stratification [e.g., Refs. [28–34]] have consistently shown a reduction of wind speed at the bottom of windward slopes, and a rapid increase towards the summit. The highest wind speeds and low-level jets are found on the crest, with a rapid decrease to below upwind speed on the lee side. These studies confirm the simplified theoretical results summarised by Smith [35]. Under conditions of stable stratification, field studies have shown that the highest wind speeds are shifted downstream from the summit to the uppermost part of the lee slope, with flow separation and return circulation occurring on the lower part [36,37]. Based on wind tunnel measurements, Ayotte and Hughes [38] showed that also in neutrally stratified flow the wind speed on the upper lee side increases with increased slope. Given these results, and considering the generally stable boundary-layer stratification, together with the prevalence of steep slopes throughout Iceland, the intensification of WRF surface winds downwind from summits and ridges appears to be physically motivated.

4. Specific locations

In this section, a more detailed overview is given of the wind energy potential of the 14 sites selected for this study (see Fig. 1). The results were obtained through high-resolution WAsP modelling, with a regular horizontal grid-spacing of 100 m, based on corrected grid-point time-series from the WRF model. In the vertical, input data is linearly interpolated between model levels to 55 mAGL, chosen as the hub height of the Enercon E44, for which turbine specific quantities are calculated. All 14 domains are about 20×20 km^2 in size. The surface roughness length over land is specified as 3 cm, whereas over water, it is set to 0.02 cm. For each site, two scenarios for different WRF model grid points are determined. Ideally, the generalisation of input data would give the same results regardless of the location of the reference point. However, in some regions, considerable differences do exist. This is indicative of the limitations of the wind atlas method, combining the limited representation of complex terrain in the mesoscale numerical model, with the highly parameterised description of boundary-layer processes in WAsP.

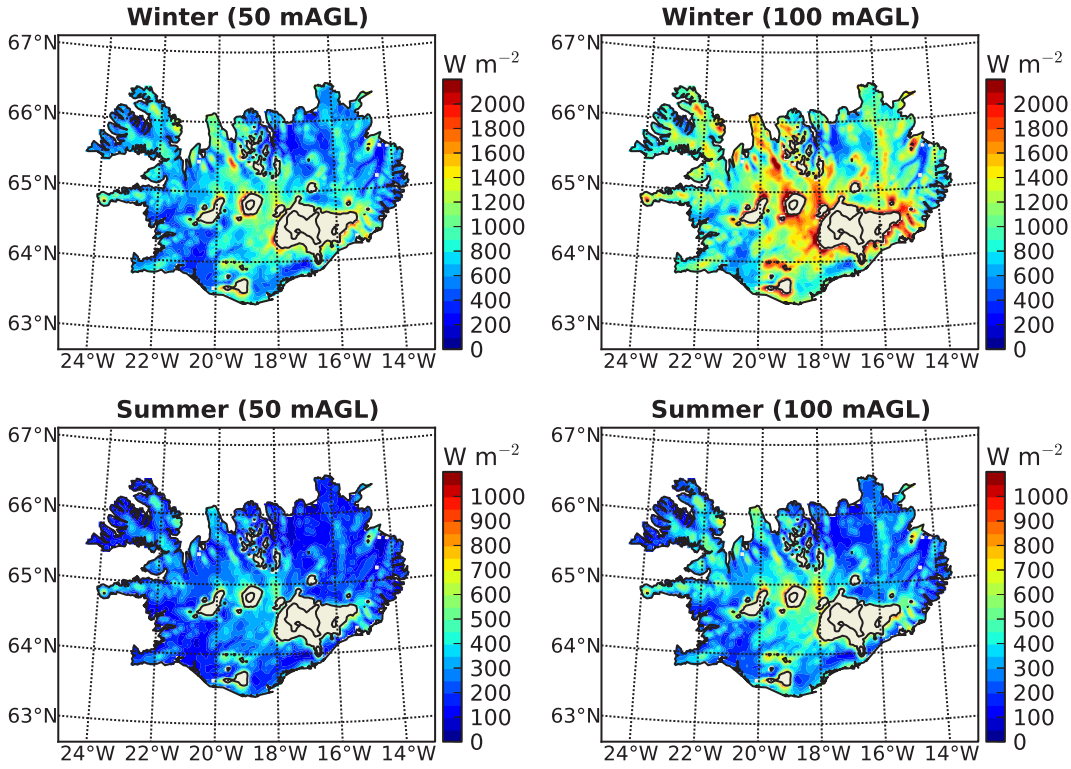

Fig. 7. Winter (DJF) and summer (JJA) averages of wind power density at 50 and 100 mAGL, based on corrected WRF model data.

For an easy overview, Table 1 lists the most relevant wind-related properties of each region. The values are spatial averages over that part of the domain within the indicated range of terrain elevation, excluding lakes. Additionally, averages were taken between the scenarios for each of the two model grid points. As seen in the previous subsections, wind conditions on Iceland are characterised by a strong seasonal cycle, with average wintertime power densities typically between 2 and 5 times higher than in summer. Wintertime increases in the actual energy production are typically between 50 and 150% of the summer averages, and are timed well with the demands for increased lighting during the winter. An interesting comparison can be made between the power density and available power on Hellisheiði and Skagi. Based on the annual wind conditions at 55 mAGL, Hellisheiði has an average power density of 1600 W m^{-2}, compared with 2530 W m^{-2} on Skagi. Therefore, purely based on atmospheric conditions, Skagi has a 58% higher wind energy potential than Hellisheiði. However, to be able to fully exploit a given wind energy potential, the cut-out speed and rated power of the chosen turbine must be sufficiently high. The saturation point of power production is reached at the

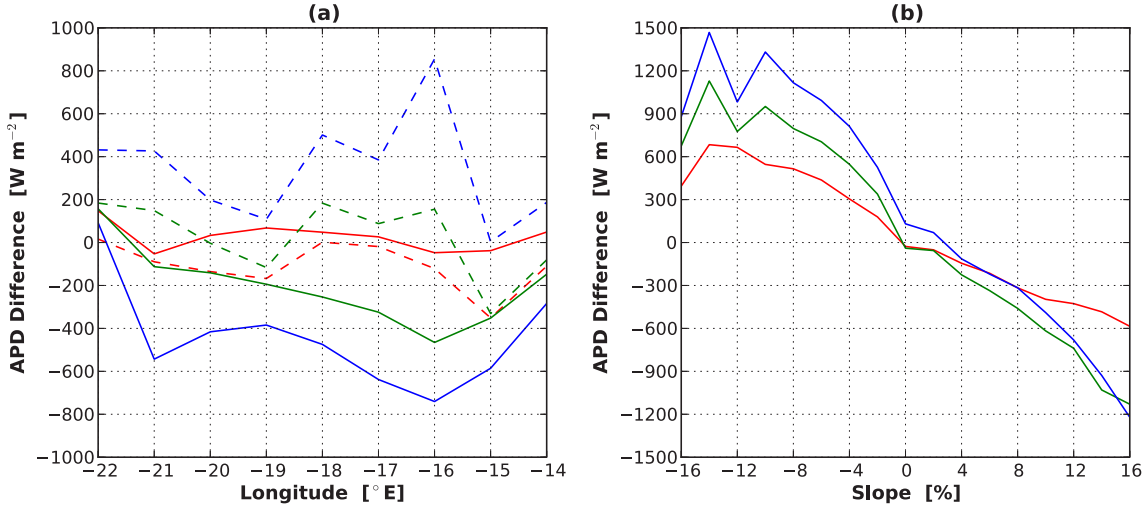

Fig. 8. Differences in average wind power density (APD) at 50 mAGL between winds from the southerly and northerly 30-degree sector (southerly minus northerly) in winter (DJF; blue lines), summer (JJA; red lines), and annually (green lines), based on corrected WRF model data. (a) APD differences along the northern (solid lines) and southern coast (dashed lines) of Iceland, as a function of longitude. (b) APD differences as a function of south-to-north terrain slope. (For interpretation of the references to colour in this figure legend, the reader is referred to the web version of this article.)

Table 1
Winter (DJF)/annual/summer (JJA) values of average power density (APD), average available power (AAP), and efficiency of power generation at 14 sites (see Fig. 1), based on the wind conditions at 55 mAGL, and for the Enercon E44 wind turbine. Maximum values of wind power and efficiency are shown in bold.

	Height [mASL]	APD [W m^{-2}]	AAP [kW]	Efficiency [%]
Blanda	450–550	2990/1610/650	510/450/320	11/19/32
Búrfell	200–400	2010/1230/510	520/440/290	17/23/38
Fljótsdalsheiði	600–700	1470/740/280	490/360/200	**22**/**32**/**46**
Gufuskálar	5–100	2370/1410/700	590/470/330	16/22/31
Hellisheiði	300–400	2210/1600/750	**630**/**540**/400	19/22/35
Höfn	5–100	1750/1070/390	460/340/180	17/21/31
Landeyjar	5–60	2140/1620/920	550/470/360	17/19/26
Langanes	5–100	1850/1130/460	570/440/260	20/26/37
Meðallandssveit	5–40	1810/1630/1200	520/500/**430**	19/20/23
Melrakkaslétta	5–100	1690/1030/450	570/440/280	**22**/28/41
Mýrar	5–20	1670/1040/460	540/430/280	21/27/40
Skagi	5–100	**4400**/**2530**/**1470**	550/480/370	8/12/17
Snæfellsnes	5–150	1690/1150/510	500/400/250	19/23/32
Þorlákshöfn	5–100	1870/1240/530	580/470/290	20/25/37

rated speed. Beyond that, efficiency is deliberately reduced to protect the turbine. At the cut-out speed and above, wind energy potential is lost completely to average available power, whereas extreme winds weigh heavily in averages of power density. In the case of Skagi, these technical limitations clearly come into play. Despite the higher values of average power density, the average available power of 480 kW is 11% lower than that on Hellisheiði, with an average available power of 540 kW. This is primarily the result of the higher proportion of above cut-out speeds, together with a small loss from a higher proportion of below cut-in speeds. Much of the power density at above-rated speeds is also lost by the reduced efficiency within that range. The average efficiency of power generation is defined here as the ratio between average available power, and average power density multiplied by the area swept by the rotor blades. As shown in the table, the efficiency on Hellisheiði is about twice as high as on Skagi.

For comparison, we performed the same calculations for the Vestas V80 (2 MW) wind turbine with a hub height of 67 m. Despite the increase in hub height, relative to the Enercon E44, the actually generated power does not increase proportional to the square of the rotor diameter, since the efficiency of larger turbines is reduced. As for the Enercon E44, the lowest efficiency is found for the wind conditions on Skagi, reduced even further for the Vestas V80 due to the 3 m s^{-1} lower cut-out speed, and 1 m s^{-1} higher cut-in speed. Not considered here is the problem of icing, which is likely to increase with greater hub heights and rotor diameters.

5. Conclusions

To be able to determine to what extent wind energy production in Iceland is viable, the annual averages of wind power density and available power need to be compared with the wind resources of other countries, as well as with the capacity of domestic hydro and geothermal power plants.

According to the European Wind Atlas published by Risø National Laboratory [10], the highest wind power class in Western Europe, not including Iceland, covers the western and northern coast of Ireland, the whole of Scotland, and the northwestern tip of Denmark. It is characterised by annual average wind power density at 50 mAGL of >250 W m^{-2} over sheltered terrain, >700 W m^{-2} along the open coast, and >1800 W m^{-2} on top of hills and ridges. Based on the results from this study, it is clear that Iceland is well within that wind power class. Annual wind conditions are therefore not a limiting factor for wind energy production. Only modest wind farms would be required to match the smallest hydropower and geothermal power plants in Iceland, with 5 and 3 MW electric capacity, respectively (see the description by Landsvirkjun of all commercial power stations in Iceland at http://www.landsvirkjun.com/Company/PowerStations/). For example, ignoring downtime due to icing and maintenance, a wind farm consisting of 15 Enercon E44 turbines installed on Hellisheiði would produce more power throughout the year than the two small power plants together.

Therefore, considering the low and reversible environmental impact from the installation of wind turbines, compared with the lasting or permanent impact especially from hydropower dams, wind power should be considered as a serious additional option for renewable energy production, especially in a country such as Iceland, with high wind energy potential, and a low population density.

Acknowledgements

This research was part of the project “Improved Forecast of Wind, Waves and Icing” (IceWind), funded by the Nordic Top-level Research Initiative (Toppforskningsinitiativet; TFI), including national and private organisations. The authors would like to thank the Institute for Meteorological Research in Iceland for the WRF model data used in this study, and the Norwegian Meteorological Institute for the NORA10 data.

References

[1] Thorsteinsson T. Renewable energy in the Nordic and Baltic countries. In: Climate change and energy systems: impacts, risks and adaptation in the Nordic and Baltic countries. Copenhagen, Denmark: Nordic Council of Ministers; 2012. pp. 27–34.
[2] Blöndal-Sveinsson ÓG, Linnet Ú, Elíasson EB. Hydropower in Iceland. Impacts and adaptation in a future climate. In: Climate change and energy systems: impacts, risks and adaptation in the Nordic and Baltic countries. Copenhagen, Denmark: Nordic Council of Ministers; 2012. pp. 27–34.
[3] Björnsson H, Jóhannesson T, Snorrason Á. Recent climate change, projected impacts and adaptation capacity in Iceland. In: Climate: global change and local adaptation. Springer; 2011. pp. 467–77.
[4] Rummukainen M, Ruosteenoia K, Kjellström E. Climate scenarios. In: Impacts of climate change on renewable energy sources: their role in the Nordic energy system. Copenhagen, Denmark: Nordic Council of Ministers; 2007. pp. 36–57.
[5] Hanna E, Cappelen J, Allan R, Jónsson T, Blanco FL, Lillington T, et al. New insights into North European and North Atlantic surface pressure variability, storminess, and related climatic change since 1830. J Clim 2008;21:6739–66.
[6] Archer CL, Jacobson MZ. Evaluation of global wind power. J Geophys Res 2005;110:D12110.
[7] Skamarock WC, Klemp JB, Dudhia J, Gill DO, Barker DM, Duda MG, et al. A description of the Advanced Research WRF Version 3. NCAR Technical Note NCAR/TN-475+STR. Boulder, Colorado, USA: National Center for Atmospheric Research; 2008.
[8] Courtier P. Dual formulation of four-dimensional variational assimilation. Q J R Meteorol Soc 1997;123:2449–61.
[9] Andersson E, Thépaut JN. ECMWF's 4D-Var data assimilation system – the genesis and ten years in operations. ECMWF Newsl 2008;115:8–12.
[10] Troen I, Petersen EL. European wind atlas. Roskilde, Denmark: Risø National Laboratory; 1989.
[11] Petersen EL, Mortensen NG, Landberg L, Højstrup J, Frank HP. Wind power meteorology. Report Risø-I-1206 (EN). Roskilde, Denmark: Risø National Laboratory; 1997.
[12] Frank HP, Landberg L. Modelling the wind climate of Ireland. Boundary-Layer Meteorol 1997;85:359–78.
[13] Mengelkamp HT, Kapitza H, Pflüger U. Statistical-dynamical downscaling of wind climatologies. J Wind Eng Ind Aerodyn 1997;67&68:449–57.
[14] Mengelkamp HT. Wind climate simulation over complex terrain and wind turbine energy output estimation. Theor Appl Climatol 1999;63:129–39.
[15] Frank HP, Rathmann O, Mortensen NG, Landberg L. The numerical wind atlas – the KAMM/WAsP method. Report Risø-R-1252 (EN). Roskilde, Denmark: Risø National Laboratory; 2001.
[16] Tammelin B, Vihma T, Atlaskin E, Badger J, Fortelius C, Gregow H, et al. Production of the Finnish wind atlas. Wind Energy 2013;16:19–35.
[17] Bowen AJ, Mortensen NG. Exploring the limits of WAsP, the wind atlas analysis and application program. In: Göteborg, Sweden: European Union Wind Energy Conference, Paper O15.2. 20–24 May 1996.
[18] Mortensen NG, Petersen EL. Influence of topographical input data on the accuracy of wind flow modelling in complex terrain. In: Dublin, Ireland: European Wind Energy Conference & Exhibition. October 1997.
[19] Ayotte KW, Davy RJ, Coppin PA. A simple temporal and spatial analysis of flow in complex terrain in the context of wind energy modelling. Boundary-Layer Meteorol 2001;98:275–95.

[20] Morgan EC, Lackner M, Vogel RM, Baise LG. Probability distributions for offshore wind speeds. Energy Convers Manage 2011;52:15–26.
[21] Seguro JV, Lambert TW. Modern estimation of the parameters of the Weibull wind speed distribution for wind energy analysis. J Wind Eng Ind Aerodyn 2000;85:75–84.
[22] Hennessey JP. Some aspects of wind power statistics. J Appl Meteorol 1977;16(2):119–28.
[23] Betz A. Introduction to the theory of flow machines. Oxford, UK: Pergamon Press; 1966. p. 281.
[24] Reistad M, Breivik O, Haakenstad H, Aarnes OJ, Furevik BR, Bidlot JR. A high-resolution hindcast of wind and waves for the North Sea, the Norwegian Sea, and the Barents Sea. J Geophys Res 2011;116:C05019.
[25] Uppala SM, Kållberg PW, Simmons AJ, Andrae U, da Costa Bechtold V, Fiorino M. The ERA-40 re-analysis. Q J R Meteorol Soc 2005;131:2961–3012.
[26] Undén P, Rontu L, Järvinen H, Lynch P, Calvo J, Cats G. HIRLAM-5 scientific documentation. Tech. Rep. Norrköping, Sweden: Swed. Meteorol. Hydrol. Inst.; 2002
[27] Beckmann P. Rayleigh distribution and its generalizations. Radio Sci J Res NBS/USNC-URSI 1964;68D(9):927–32.
[28] Walmsley JL, Taylor PA. Boundary-layer flow over topography: impacts of the Askervein study. Boundary-Layer Meteorol 1996;78(3–4):291–320.
[29] Apsley DD, Castro IP. Flow and dispersion over hills: comparison between numerical predictions and experimental data. J Wind Eng Ind Aerodyn 1997;67&68:375–86.
[30] Takahashia T, Ohtsua T, Yassina M, Katoa S, Murakami S. Turbulence characteristics of wind over a hill with a rough surface. J Wind Eng Ind Aerodyn 2002;90:1697–706.
[31] Takahashia T, Katoa S, Murakamib S, Ookaa R, Yassinc MF, Kono R. Wind tunnel tests of effects of atmospheric stability on turbulent flow over a three-dimensional hill. J Wind Eng Ind Aerodyn 2005;93:155–69.
[32] Corbett JF, Ott S, Landberg L. A mixed spectral-integration model for neutral mean wind flow over hills. Boundary-Layer Meteorol 2008;128:229–54.
[33] Lewis HW, Mobbs SD, Lehning M. Observations of cross-ridge flows across steep terrain. Q J R Meteorol Soc 2008;134:801–16.
[34] Moreira GAA, dos Santos AAC, do Nascimento CAM, Valle RM. Numerical study of the neutral atmospheric boundary layer over complex terrain. Boundary-Layer Meteorol 2012;143:393–407.
[35] Smith RB. Hydrostatic airflow over mountains. Adv Geophys 1989;31:1–41.
[36] Vosper SB, Mobbs SD, Gardiner BA. Measurements of the near-surface flow over a hill. Q J R Meteorol Soc 2002;128:2257–80.
[37] Barkwith A, Collier CG. Lidar observations of flow variability over complex terrain. Meteorol Appl 2011;18:372–82.
[38] Ayotte KW, Hughes DE. Observations of boundary-layer wind-tunnel flow over isolated ridges of varying steepness and roughness. Boundary-Layer Meteorol 2004;112:525–56.